

Contribution from the Department of Chemistry,
Faculty of Science, Hiroshima University, Hiroshima 730, Japan

Structure, Thermal Racemization, and Ion Association of the [1,1,1-Tris(5-amino-2-azapentyl)ethane]cobalt(III) Complex

USHIO SAKAGUCHI,[†] KANJI TOMIOKA, TAKAKI KASHIHARA, and HAYAMI YONEDA*

Received March 22, 1984

The structure of $[\text{Co}(\text{stn})\text{Cl}_3 \cdot 3.5\text{H}_2\text{O}$ (stn = 1,1,1-tris(5-amino-2-azapentyl)ethane) has been determined by single-crystal X-ray techniques ($R = 0.0585$, monoclinic crystals, space group $C2/c$ with $a = 29.038$ (10) Å, $b = 10.971$ (5) Å, $c = 14.763$ (3) Å, $\beta = 99.861$ (23)°, and $Z = 8$). The cation has a rather strained geometry, and the three six-membered chelate rings are in a flattened-chair conformation. The rate of racemization of the cation has been measured both in solids and in solution and a novel racemization mechanism proposed. Association constants of Λ - $[\text{Co}(\text{stn})]^{3+}$ with *d*- and *l*-tartrate, bis(μ -*d*-tartrato)- and bis(μ -*l*-tartrato)diantimonate(III), and sulfate ions have been measured, and their mode of association has been discussed.

Introduction

We have been interested in the effect of covalent capping on cobalt(III) amine complexes.¹⁻⁵ Capping along the C_3 axis of $[\text{Co}(\text{en})_3]^{3+}$ (en = ethylenediamine), yielding $[\text{Co}(\text{sen})]^{3+}$ (sen = 1,1,1-tris(4-amino-2-azabutyl)ethane) illustrated in Figure 1, produced no significant strain in its structure but did produce interesting chemical properties.^{1,2,6} Capping along the pseudo- C_3 axis of $[\text{Co}(\text{en})_3]^{3+}$, forming the complex $[\text{Co}(\text{L})(\text{en})]^{3+}$ with the novel ligand L = 6-methyl-6-(4-amino-2-azabutyl)-1,4-diazacycloheptane, imparted severe steric strain and a remarkable change in spectroscopic properties.³ The complex $[\text{Co}(\text{stn})]^{3+}$ (stn = 1,1,1-tris(5-amino-2-azapentyl)ethane, $\text{CH}_3\text{C}(\text{CH}_2\text{NHCH}_2\text{CH}_2\text{CH}_2\text{NH}_2)_3$) has such a structure that a trimethyleneethane group is capped along the C_3 axis of $[\text{Co}(\text{tn})]^{3+}$ (tn = 1,3-propanediamine), as shown in Figure 1, and was prepared previously by Hermer and Douglas⁷ and recently by Geue and Searle.⁸ Optical resolution was also effected by the former authors. However, their method of synthesis as well as of optical resolution was inefficient, especially for large-scale synthesis. In this paper, the preparation and optical resolution of $[\text{Co}(\text{stn})]^{3+}$ and the structure determination of $[\text{Co}(\text{stn})\text{Cl}_3 \cdot 3.5\text{H}_2\text{O}$ are described. Further, the chiral form of the cation was found to racemize thermally both in solids and in solution. On the basis of kinetic studies, a novel racemization mechanism is proposed.

Experimental Section

Preparation of $[\text{Co}(\text{stn})]^{3+}$. 1,1,1-Tris(hydroxymethyl)ethane was tosylated in pyridine by the method of Hein and Burkhardt.⁹ The tritosylate (100 g) was refluxed with a large excess of anhydrous tn (500 g) for 72 h out of contact with atmospheric moisture and carbon dioxide. Excess tn was removed by a rotary evaporator, a solution of sodium hydroxide (240 g) in water (400 mL) was added to the viscous yellow residue, and this then was extracted three times with pyridine (1 L). The extracts were rotary evaporated to give a viscous yellow oil, to which 300 mL of ethanol was added. The mixture was suction filtered to remove *p*-toluenesulfonic acid salts, and this ethanolic solution of crude stn was used directly in the subsequent reaction.

Sixty grams of *trans*- $[\text{CoCl}_2(\text{py})_4]\text{Cl}^{10}$ (py = pyridine) in 1 L of warm methanol was added, with stirring, to the above ethanol solution of stn. The resulting rose pink precipitate of $[\text{Co}(\text{stn})\text{Cl}_3 \cdot 3.5\text{H}_2\text{O}$ was suction filtered and recrystallized from warm water. The overall yield based on the starting material 1,1,1-tris(hydroxymethyl)ethane was about 60%. Anal. Calcd for $[\text{Co}(\text{C}_{14}\text{H}_{36}\text{N}_6)]\text{Cl}_3 \cdot 5\text{H}_2\text{O}$: C, 32.54; N, 16.26; H, 8.39. Found: C, 32.25; N, 16.00; H, 8.17. The perchlorate salt was obtained by adding solid sodium perchlorate to an aqueous solution of the chloride. Anal. Calcd for $[\text{Co}(\text{C}_{14}\text{H}_{36}\text{N}_6)](\text{ClO}_4)_3$: C, 26.04; N, 13.01; H, 5.62. Found: C, 26.05; N, 12.95; H, 5.85. The iodide salt was obtained similarly by using NaI instead of NaClO_4 . Anal. Calcd for $[\text{Co}(\text{C}_{14}\text{H}_{36}\text{N}_6)]\text{I}_3 \cdot \text{H}_2\text{O}$: C, 22.53; N, 11.26; H, 5.14. Found: C, 22.42; N, 11.19; H, 5.18.

Optical Resolution of $[\text{Co}(\text{stn})]^{3+}$. Optical resolution of $[\text{Co}(\text{stn})]^{3+}$ was effected by the use of the optically active $[\text{Co}(\text{ox})_3]^{3-}$ (ox = oxalate),¹¹ which had been prepared from the optically active $[\text{Co}(\text{en})_3]^{3+}$ · H_2O . The less soluble diastereomer with a combination of Δ - $[\text{Co}(\text{stn})]$ and Λ - $[\text{Co}(\text{ox})_3]$ that precipitated out was filtered, dissolved

in a large volume of water, and applied to an ion-exchange column of SP-Sephadex C-25 (Na^+ form). Elution with 0.5 M sodium perchlorate and concentration of the effluent on a rotary evaporator at temperatures below 40 °C yielded the perchlorate salt. The filtrate obtained by removing the less soluble diastereomer was treated similarly. Both enantiomers were recrystallized from warm water (acidified slightly by perchloric acid) to a constant rotation. Anal. Calcd for $[\text{Co}(\text{C}_{14}\text{H}_{36}\text{N}_6)](\text{ClO}_4)_3$: C, 26.04; N, 13.01; H, 5.62. Found: C, 26.16; N, 12.99; H, 5.88. The circular dichroism (CD) spectrum in water had peaks at 521 ($\Delta\epsilon = +0.514$), 462 (-0.070), and 369 ($+0.0925$) nm.

Measurements. Electronic absorption and CD spectra were obtained on a Shimadzu UV-240 double-beam spectrophotometer and a JASCO J-40CS recording spectropolarimeter, respectively. Optical rotations were measured on a Union Giken PM-71 polarimeter at ambient temperatures.

Racemization rates in solution were measured in 5×10^{-2} M 2,4,6-collidine buffered solutions (pH 6.73–7.96) at temperatures of 55.0, 60.0, 65.0, and 70.0 °C maintained by a Haake circulator. Racemization rates in the solid state were obtained by heating solid samples put in glass tubes in an Abderhalden apparatus at refluxing temperatures of water, ethanol, norbornadiene, and an azeotropic mixture of 2-butanol and toluene (55%:45%).

Association constants with *d*- and *l*-tartrate, bis(μ -*d*-tartrato)- and bis(μ -*l*-tartrato)diantimonate(III), and sulfate ions were measured at 25.0 °C by the method described in previous papers.^{2,5} The complex concentration was set to 1.0×10^{-3} M, and the concentration of the anions was changed from 0 to 3.13×10^{-2} M for tartrate systems and from 0 to 2.50×10^{-2} M for the other. Ionic strength was adjusted to $\mu = 0.1$ with sodium perchlorate.

Collection of the X-ray Diffraction Data of $[\text{Co}(\text{stn})\text{Cl}_3 \cdot 3.5\text{H}_2\text{O}$. A red crystal of $[\text{Co}(\text{C}_{14}\text{H}_{36}\text{N}_6)]\text{Cl}_3 \cdot 3.5\text{H}_2\text{O}$ with the dimensions $0.50 \times 0.13 \times 0.25$ mm was used for the data collection. The cell constants were determined from Eissenberg photographs taken with Ni $K\alpha$ radiation and refined with reflection data collected at 20 °C on a Syntex R3 automated four-circle diffractometer utilizing Mo $K\alpha$ radiation made monochromatic with a graphite plate ($\lambda = 0.71069$ Å). The possible space groups deduced from the systematic absences for hkl ($h + k = 2n$), $h0l$ ($l = 2n$ and $h = 2n$), and $0k0$ ($k = 2n$) are Cc (No. 9) and $C2/c$ (No. 15). The cell constants, determined by a least-squares method using 13 independent reflections with $14.89^\circ < 2\theta < 23.35^\circ$, were $a = 29.038$ (10) Å, $b = 10.971$ (5) Å, $c = 14.763$ (3) Å, $\beta = 99.861$ (23)°, and $V = 4633.83$ (269) Å³. The measured density of 1.27 g cm⁻³ obtained by the flotation method using a CHBr_3 - $\text{C}_2\text{H}_5\text{OH}$ mixed solution agreed well with the calculated value of 1.267 g cm⁻³ for $Z = 8$. The intensity data were

- (1) Okazaki, H.; Sakaguchi, U.; Yoneda, H. *Inorg. Chem.* **1983**, *22*, 1539–1542.
- (2) (a) Sakaguchi, U.; Tsuge, A.; Yoneda, H. *Inorg. Chem.* **1983**, *22*, 1630–1634. (b) Sakaguchi, U.; Tsuge, A.; Yoneda, H. *Inorg. Chem.* **1983**, *22*, 3745–3749.
- (3) (a) Sakaguchi, U.; Tomioka, K.; Yoneda, H. *Chem. Lett.*, in press. (b) Tomioka, K.; Sakaguchi, U.; Yoneda, H. *Inorg. Chem.* **1984**, *23*, 2863.
- (4) Tomioka, K.; Sakaguchi, U.; Yoneda, H., submitted for publication.
- (5) Sakaguchi, U.; Tamaki, S.; Tomioka, K.; Yoneda, H., submitted for publication.
- (6) Sarneski, J. E.; Urbach, F. L. *J. Am. Chem. Soc.* **1971**, *93*, 884–888.
- (7) Hermer, R. E.; Douglas, B. E. *J. Coord. Chem.* **1977**, *7*, 43–52.
- (8) Geue, R. J.; Searle, G. H. *Aust. J. Chem.* **1983**, *31*, 927–935.
- (9) Hein, F.; Burkhardt, R. *Chem. Ber.* **1957**, *90*, 928–935.
- (10) Werner, A.; Feenstra, R. *Ber. Dtsch. Chem. Ges.* **1906**, *39*, 1538–1545.
- (11) (a) Vaughn, J. W.; Magnuson, V. E.; Seiler, G. J. *Inorg. Chem.* **1969**, *8*, 1201–1202. (b) Butler, K. R.; Snow, M. R. *J. Chem. Soc., Dalton Trans.* **1976**, 251–258.

[†] Present address: Kumamoto University of Commerce, Ooe-2-5-1, Kumamoto 862, Japan.

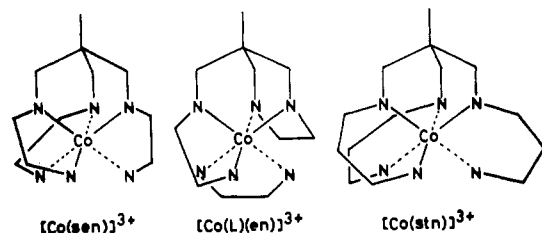


Figure 1. Schematic illustration of the complexes.

Table I. Positional Parameters ($\times 10^5$)

| atom | x | y | z |
|------|-------------|--------------|--------------|
| Co | 11 089 (2) | 17 189 (4) | 13 753 (3) |
| N1 | 15 481 (10) | 4 113 (28) | 11 056 (20) |
| N2 | 7 519 (11) | 6 240 (29) | 20 769 (22) |
| N3 | 14 643 (11) | 29 062 (29) | 7 329 (21) |
| N4 | 6 823 (11) | 12 307 (30) | 2 413 (21) |
| N5 | 15 404 (11) | 20 902 (28) | 25 562 (20) |
| N6 | 6 544 (12) | 30 345 (30) | 15 206 (24) |
| C0 | 27 109 (15) | 20 120 (53) | 17 495 (36) |
| C1 | 21 775 (13) | 19 256 (38) | 16 313 (26) |
| C2 | 20 389 (13) | 5 815 (38) | 15 821 (26) |
| C3 | 14 105 (15) | -9 022 (35) | 11 099 (27) |
| C4 | 11 903 (15) | -12 773 (35) | 19 162 (28) |
| C5 | 7 201 (14) | -7 033 (36) | 18 954 (27) |
| C6 | 19 648 (13) | 25 750 (37) | 7 430 (27) |
| C7 | 12 507 (17) | 34 414 (47) | -1 716 (32) |
| C8 | 10 015 (18) | 25 757 (46) | -8 470 (32) |
| C9 | 5 615 (16) | 20 707 (41) | -5 508 (29) |
| C10 | 20 129 (14) | 25 305 (38) | 24 452 (26) |
| C11 | 13 683 (16) | 27 995 (42) | 33 072 (27) |
| C12 | 10 827 (19) | 38 902 (41) | 29 766 (33) |
| C13 | 6 196 (17) | 35 547 (38) | 24 347 (32) |
| C11 | -3 074 (4) | 11 664 (10) | 9 970 (8) |
| C12 | 17 728 (5) | 5 (11) | 40 696 (7) |
| C13 | 16 076 (10) | 56 375 (21) | 12 131 (19) |
| O1 | 0 (0) | 66 143 (39) | 25 000 (0) |
| O2A | 44 007 (21) | 9 213 (54) | 40 563 (50) |
| O2B | 43 124 (52) | 14 127 (113) | 48 905 (107) |
| O3 | 73 210 (22) | -13 059 (73) | 50 760 (48) |
| O4 | 50 480 (23) | 313 (49) | 43 113 (45) |

measured for $+h, +k, \pm l$ ($h + k = 2n + 1$) up to $2\theta = 55^\circ$ by the ω -scan technique with a scan speed of $3\text{--}29.3^\circ \text{ min}^{-1}$ (50 kV, 20 mA). Three reference reflections monitored after every cycle of 200 measurements showed no significant variation in intensity during the data collection. Out of 5412 unique reflections measured, 4503 reflections with $|F_o| > 3\sigma(|F_o|)$ were used for the structure determination. They were corrected for Lorentz-polarization factors, but no absorption correction was applied since the linear absorption coefficient of $\mu(\text{Mo K}\alpha) = 12.5 \text{ cm}^{-1}$ was low.

Structure Determination and Refinement. Since the Wilson statistics of the data indicated the presence of a symmetry center, the structure was solved in space group $C2/c$. The position of the Co atom was located by using the results of MULTAN direct-method analysis (MULTAN 78¹²). All other computations were carried out with use of the Universal Crystallographic Computation Program System, UNICS III.¹³ Subsequent difference Fourier maps revealed the positions of the remaining non-hydrogen atoms. After all the non-hydrogen atoms were refined isotropically, a series of refinements using anisotropic thermal parameters for all non-hydrogen atoms reduced the R_1 value ($= \sum(|F_o| - |F_c|) / \sum|F_o|$) to 0.0827 and the R_w value ($= [\sum(|F_o| - |F_c|)^2 / \sum|F_o|^2]^{1/2}$) to 0.1067. All the hydrogen atoms except those of water molecules were located from subsequent difference Fourier maps. Further refinements without hydrogen atoms of water molecules, using anisotropic thermal parameters for all non-hydrogen atoms and isotropic thermal parameters for hydrogen atoms, reduced R_1 to 0.0663 and R_w ($= [\sum w(|F_o| - |F_c|)^2 / \sum w|F_o|^2]^{1/2}$) to 0.0850. The difference Fourier map at this stage showed a large peak ($2.18 \text{ e}/\text{\AA}^3$) near O2 (one of the oxygen atoms of the water molecules), and the oxygen atom was placed on the two positions with

Table IV. Intramolecular Bond Distances (\AA) with Least-Squares Estimated Standard Deviations in Parentheses

| | | | |
|---------|-----------|---------|-----------|
| Co-N1 | 2.004 (3) | Co-N2 | 1.990 (3) |
| Co-N3 | 1.999 (3) | Co-N4 | 1.983 (3) |
| Co-N5 | 2.012 (3) | Co-N6 | 1.992 (4) |
| N1-C2 | 1.491 (5) | N1-C3 | 1.496 (5) |
| N2-C5 | 1.481 (5) | N3-C6 | 1.495 (5) |
| N3-C7 | 1.497 (5) | N4-C9 | 1.486 (5) |
| N5-C10 | 1.489 (5) | N5-C11 | 1.509 (6) |
| N6-C13 | 1.487 (6) | C0-C1 | 1.531 (6) |
| C1-C2 | 1.527 (6) | C1-C6 | 1.530 (5) |
| C1-C10 | 1.521 (6) | C3-C4 | 1.503 (6) |
| C4-C5 | 1.499 (6) | C7-C8 | 1.476 (7) |
| C8-C9 | 1.523 (7) | C11-C12 | 1.491 (7) |
| C12-C13 | 1.490 (7) | | |

Table V. Intramolecular Bond Angles (deg) with Least-Squares Estimated Standard Deviations in Parentheses

| | | | |
|------------|-----------|-------------|-----------|
| N1-Co-N2 | 94.4 (1) | N1-Co-N6 | 174.8 (1) |
| N2-Co-N3 | 176.1 (1) | N3-Co-N4 | 94.2 (1) |
| N4-Co-N5 | 175.9 (1) | N5-Co-N6 | 94.9 (1) |
| Co-N1-C2 | 113.9 (2) | Co-N1-C3 | 120.7 (3) |
| Co-N2-C5 | 121.4 (3) | Co-N3-C6 | 114.5 (2) |
| Co-N3-C7 | 120.8 (3) | Co-N4-C9 | 122.0 (3) |
| Co-N5-C10 | 114.8 (2) | Co-N5-C11 | 120.6 (2) |
| Co-N6-C13 | 121.6 (3) | C0-C1-C2 | 108.6 (4) |
| C0-C1-C6 | 108.8 (4) | C0-C1-C10 | 109.2 (3) |
| C2-C1-C6 | 110.1 (3) | C2-C1-C10 | 110.1 (3) |
| C6-C1-C10 | 110.0 (3) | N1-C2-C1 | 111.5 (3) |
| N1-C3-C4 | 114.6 (3) | C3-C4-C5 | 112.1 (3) |
| N2-C5-C4 | 112.4 (3) | N3-C6-C1 | 111.9 (3) |
| N3-C7-C8 | 115.7 (4) | C7-C8-C9 | 112.2 (4) |
| N4-C9-C8 | 110.8 (3) | N5-C10-C1 | 111.3 (3) |
| N5-C11-C12 | 114.1 (3) | C11-C12-C13 | 112.3 (4) |
| N6-C13-C12 | 113.0 (4) | | |

a respective weight of 0.5. The final refinement converged R_1 to 0.0585 and R_w to 0.0746. The weighting scheme used was as follows: for $|F_o| < 15$, $w = 0.7$; for $15 < |F_o| < 100$, $w = 1.0$; for $|F_o| > 100$, $w = (100.0/|F_o|)^2$. The largest residuals 1.53 and $1.26 \text{ e}/\text{\AA}^3$ in the final difference Fourier map are located near C7 and O1 atoms, respectively. Since the other residuals were less than $0.83 \text{ e}/\text{\AA}^3$, the positions of hydrogen atoms of water molecules were not determined.

All the scattering factors were taken from the tables of Cromer and Waber.¹⁴ The anomalous dispersion coefficients of Cromer and Liberman¹⁵ were used for Co and C1. The final atomic coordinates for non-hydrogen and hydrogen atoms and final thermal parameters are given in Tables I-III, respectively, according to the atom labels of Figure 2 (Tables II and III are supplementary material). All the computations, including ORTEP drawings,¹⁶ were carried out by a HITAC M-200 computer at the Hiroshima University Information Processing Center. A table of observed and calculated structure factor amplitudes is available as supplementary material.

Results

Description of the Structure of $[\text{Co}(\text{stn})]\text{Cl}_3 \cdot 3.5\text{H}_2\text{O}$. The structure of the cation with atom labels is given in Figure 2 as a stereopair. The bond lengths and angles are given in Tables IV and V, respectively. The cation has an approximate threefold axis of rotation. The geometry of the trimethyleneethane capping group is very close to that in $\Delta\text{-}[\text{Co}(\text{sen})]\text{Cl}(d\text{-C}_4\text{H}_4\text{O}_6) \cdot 6\text{H}_2\text{O}$.¹ The three six-membered chelate rings are all in a flattened-chair form; the chairs are flattened out significantly along the N...N line, and this flattening is more prominent about the secondary nitrogens rather than the primary ones. The Co-N bond length tends to be longer for secondary nitrogens. The chelate bite angles (average $94.5 (4)^\circ$) are rather large for six-membered chelate rings (see below).

Hydrogen bond distances less than 3.52 \AA are summarized in Table VI (supplementary material). In the crystal, amine hy-

(12) Main, P.; Hull, S. E.; Lessinger, L.; Germain, G.; Declercq, J. P.; Woolfson, M. M. "MULTAN: A System of Computer Programs for the Automatic Solution of Crystal Structures from X-ray Diffraction Data"; Universities of York, England, and Louvain, Belgium, 1978.
 (13) Sakurai, T.; Kobayashi, K. *Rikagaku Kenkyusho Hokoku* 1979, 55, 69-77.

(14) Cromer, D. T.; Waber, J. T. "International Tables for X-ray Crystallography"; Kynoch Press: Birmingham, England, 1974; Vol. IV, pp 72-79.
 (15) Cromer, D. T.; Liberman, D. *J. Chem. Phys.* 1970, 53, 1891-1898.
 (16) Johnson, C. K. *Oak Ridge Natl. Lab., [Rep.] ORNL (U.S.)* 1976, ORNL-5138.

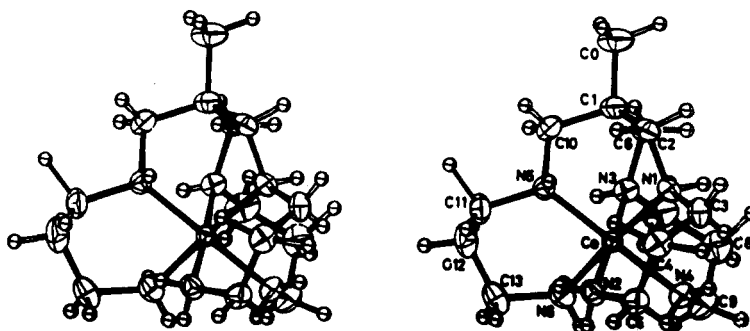


Figure 2. Stereoscopic drawing of the cation with atom labels. Thermal ellipsoids are drawn to include 50% of probability distribution.

Table VII. Racemization Rates of Λ -[Co(stn)]³⁺

| temp, °C | pH ^a | 10 ⁵ k _{obsd} , s ⁻¹ | k, M ⁻¹ s ⁻¹ | k _{av} , M ⁻¹ s ⁻¹ |
|----------|-----------------|---|------------------------------------|---|
| 55.0 | 7.86 | 22.6 | 309.0 | (2.87 ± 0.14) × 10 ² |
| | 7.70 | 14.0 | 281.8 | |
| | 7.52 | 9.59 | 288.4 | |
| | 7.30 | 5.38 | 272.3 | |
| | 7.09 | 3.44 | 281.8 | |
| 60.0 | 7.64 | 33.9 | 776.2 | (7.24 ± 0.52) × 10 ² |
| | 7.48 | 22.7 | 767.4 | |
| | 7.28 | 13.7 | 724.4 | |
| | 7.00 | 7.02 | 707.9 | |
| | 6.73 | 3.46 | 645.7 | |
| 65.0 | 7.96 | 108 | 1175 | (1.27 ± 0.08) × 10 ³ |
| | 7.68 | 60.1 | 1259 | |
| | 7.61 | 49.8 | 1230 | |
| | 7.44 | 34.8 | 1259 | |
| | 7.19 | 19.3 | 1259 | |
| | 6.90 | 11.3 | 1412 | |
| 70.0 | 7.84 | 182 | 2630 | (2.63 ± 0.04) × 10 ³ |
| | 7.71 | 137 | 2690 | |
| | 7.44 | 71.8 | 2630 | |
| | 7.19 | 39.8 | 2570 | |
| | 6.90 | 20.8 | 2630 | |

^a 5.0 × 10⁻² M collidine buffers.

drogens are bonded weakly to mostly chloride ions, and it is only one of the two N6 hydrogens that apparently hydrogen bonds to oxygen atoms.

Thermal Racemization. Racemization studies were performed both in solids and in solution. In phosphate, borate/acetate, and diethylbarbiturate/acetate buffers, decomposition of the complex ion was observed. The fact that racemization in collidine buffers was not accompanied by decomposition was confirmed by absorption, ¹H NMR, and CD spectra and by ion-exchange chromatography on SP-Sephadex C-25 column (Na⁺ form). The racemization in 5 × 10⁻² M collidine buffers followed the rate law of the form k_{obsd} = k[OH⁻], where k_{obsd} is the observed pseudo-first-order rate constant and k is the second-order rate constant. The rate constants are listed in Table VII. From the temperature dependence of k values, the activation enthalpy and entropy for racemization were determined at ΔH[‡] = 132 ± 6 kJ mol⁻¹ and ΔS[‡] = +204 ± 18 J K⁻¹ mol⁻¹.

The racemization in the solid state was studied for the anhydrous perchlorate salt only, because the chloride and bromide salts decomposed appreciably during racemization. The racemization of the perchlorate salt accompanied no decomposition, which was confirmed by UV/vis spectra and ion-exchange chromatography. The change with time in the optical activity of Λ -[Co(stn)](ClO₄)₃ is given in Figure 3 and appears to consist of two stages. The second slower rate process could be described by a simple exponential law, as is evident from the figure, but the first rapid process could not. The rate constants for the second process were 3.47 × 10⁻⁷, 5.67 × 10⁻⁷, 7.82 × 10⁻⁷, and 1.32 × 10⁻⁶ s⁻¹ at 78.2, 89.8, 96.0, and 99.2 °C, respectively. The activation parameters for this process were ΔH[‡] = 60 ± 4 kJ mol⁻¹ and ΔS[‡] = -200 ± 26 J K⁻¹ mol⁻¹. The percentage of optical activity lost in the first process was greater at higher temperatures. The percentage of optically active [Co(stn)](ClO₄)₃ pertaining

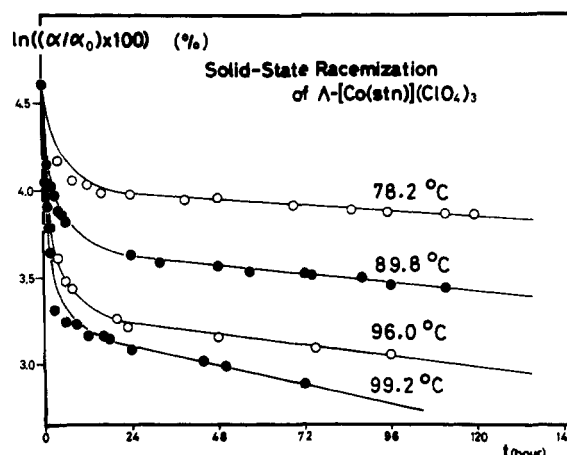


Figure 3. Solid-state racemization of Λ -[Co(stn)](ClO₄)₃. The ordinate is ln(100α/α₀), where α₀ and α are the optical activities at times zero and t, respectively.

Table VIII. Association Constants of Λ -[Co(stn)]³⁺ at 25.0 °C and μ = 0.1 (NaClO₄)^a

| anion | λ, nm | K, M ⁻¹ | Δε _{MA} | Δε _M |
|---|-------|--------------------|------------------|-----------------|
| <i>d</i> -tart ²⁻ | 380 | 41 ± 2 | 0.025 | 0.072 |
| <i>l</i> -tart ²⁻ | 380 | 22 ± 1 | 0.004 | 0.072 |
| [Sb ₂ (<i>d</i> -tart) ₂] ²⁻ | 480 | 40 ± 2 | 0.123 | 0.0 |
| [Sb ₂ (<i>l</i> -tart) ₂] ²⁻ | 480 | 30 ± 2 | 0.100 | 0.0 |
| SO ₄ ²⁻ | 480 | 146 ± 6 | -0.070 | 0.0 |

^a Abbreviations: *d*-tart²⁻ = *d*-tartrate ion; [Sb₂(*d*-tart)₂]²⁻ = bis(μ-*d*-tartrato)diantimonate(III) ion.

to the second process, obtained by extrapolation to zero time, was about 55, 39, 27, and 25% at (78.2, 89.8, 96.0, and 99.2 °C, respectively).

Ion Association. The effects of ion association on the CD spectrum of Λ -[(stn)]³⁺ were examined for *d*- and *l*-tartrate, bis(μ-*d*-tartrato)- and bis(μ-*l*-tartrato)diantimonate(III), and sulfate ions. From CD changes due to these ions, the association constants, as well as the CD curves of fully ion-paired species, were obtained. The CD curves and association constants obtained are given in Figure 5 and Table VIII, respectively.

Discussion

The preparation and optical resolution of [Co(stn)]³⁺ were first reported by Hermer and Douglas.⁷ Their methods are, however, tedious, as noted recently by Geue and Searle⁸ and us.³ Thus, the ligand stn was prepared in this work by a method similar to that used for sen. Briefly, it involves the tosylation of 1,1,1-tris(hydroxymethyl)ethane, followed by reflux of the tritosylate in a large excess of tn, and extraction with pyridine. This crude stn was used directly in subsequent reactions, because it was rather difficult to completely separate stn from the reaction mixture by distillation. The crude stn reacted smoothly with *trans*-[CoCl₂(py)₄]Cl in methanol, and rose pink crystals of the chloride salt precipitated in good yield. The above method for the synthesis of the ligand is essentially similar to the method of Geue and

Searle. The present method seems to be convenient and to be especially suited for large-scale synthesis. The electronic absorption spectrum of $[\text{Co}(\text{stn})](\text{ClO}_4)_3$ in water had peaks at 492 ($\epsilon = 82$), 356 (97), and 242 (239 990) nm. The ϵ values reported previously⁷ are much larger, which may have resulted from charge-transfer contributions of iodide ions that were used as counterions. The present method of optical resolution that employs optically active $[\text{Co}(\text{ox})_3]^{3-}$ is also much more efficient than the method reported. The CD spectrum of the optically pure complex agreed with that reported.⁷

Structural Features. The structures of $[\text{Co}(\text{N})_6]^{3+}$ complexes containing three six-membered chelate rings have been reported for $[\text{Co}(\text{tn})_3]^{3+}$,¹⁷ Δ -*fac*- $[\text{Co}(\text{R},\text{S}\text{-ptn})_3]^{3+}$ (ptn = 2,4-pentanediamine),¹⁸ Δ -*ob*₃- $[\text{Co}(\text{R},\text{R}\text{-ptn})_3]^{3+}$,¹⁹ and Δ -*lel*₃- $[\text{Co}(\text{R},\text{R}\text{-ptn})_3]^{3+}$.²⁰ However, detailed comparison of the structures was frustrated by the fact that structural parameters reported previously are all scattered from one chelate ring to another. Thus, only qualitative comparison is given in the following. (1) The chair form of tn rings in $[\text{Co}(\text{stn})]^{3+}$ appears to be the most flattened. This can be seen in the dihedral angles D1 and D2 of 159.4 (2) and 117.7 (3)°, respectively, where D1 is the dihedral angle between the NCoN and NCCN planes and D2 the dihedral angle between the CCC and NCCN planes. The D1 and D2 angles of $[\text{Co}(\text{tn})_3]^{3+}$ and Δ -*fac*- $[\text{Co}(\text{R},\text{S}\text{-ptn})_3]^{3+}$ are 150.6 (36) and 122.1 (26)°, and 150.5 (62) and 121.6 (37)°, respectively. The flattening can also be seen in the Co-N-C-C and N-Co-N-C torsional angles. In $[\text{Co}(\text{stn})]^{3+}$, the Co-N-C-C angle is 45.0 (8)° (near the cap) and 51.1 (24)° (for the other) and the N-Co-N-C angle is 22.1 (17)° (near the cap) and 25.8 (3)°. The differences between 45.0 and 51.1°, and between 22.1 and 25.8°, point to the chair form being more flattened about secondary nitrogens. For comparison, the Co-N-C-C and N-Co-N-C angles in $[\text{Co}(\text{tn})_3]^{3+}$ and Δ -*fac*- $[\text{Co}(\text{R},\text{S}\text{-ptn})_3]^{3+}$ are 53.8 (32) and 34.8 (50)°, and 53.8 (22) and 35.9 (12)°, respectively. (2) The Co-N-C angles of 120.7 (1)° (near the cap) and 121.7 (3)° (for the other) of $[\text{Co}(\text{stn})]^{3+}$ are close to 122.2 (7), 123.2 (11), 115.7 (14) and 118.0 (9)° for $[\text{Co}(\text{tn})_3]^{3+}$, Δ -*fac*- $[\text{Co}(\text{R},\text{S}\text{-ptn})_3]^{3+}$, Δ -*ob*₃- $[\text{Co}(\text{R},\text{R}\text{-ptn})_3]^{3+}$, and Δ -*lel*₃- $[\text{Co}(\text{R},\text{R}\text{-ptn})_3]^{3+}$, in this order. (3) The N-Co-N angle of 94.5 (4)° of $[\text{Co}(\text{stn})]^{3+}$ appears to be larger than that of the other six-membered chelates. For comparison, the angles in $[\text{Co}(\text{tn})_3]^{3+}$, Δ -*ob*₃- $[\text{Co}(\text{R},\text{R}\text{-ptn})_3]^{3+}$, Δ -*fac*- $[\text{Co}(\text{R},\text{S}\text{-ptn})_3]^{3+}$, and Δ -*lel*₃- $[\text{Co}(\text{R},\text{R}\text{-ptn})_3]^{3+}$ are 90.4 (1), 88.3 (15), 89.9 (25), and 89.1 (3)°, respectively.

All these tendencies suggest that the six-membered chelate rings in $[\text{Co}(\text{stn})]^{3+}$ are the most strained. To establish this point unequivocally, a comparative study using conformational analysis will be needed.

The chair₃ conformation found seems to be the only possibility for $[\text{Co}(\text{stn})]^{3+}$. Other conformation such as boat₃, *ob*₃, and *lel*₃ or intermediates between these appear improbable from consideration of molecular models, owing to the production of severe nonbonded interactions between hydrogens. This inference suggests that the conformation of $[\text{Co}(\text{stn})]^{3+}$ in solution remains intact and this suggestion, in turn, is consistent with the observation that the CD spectrum of Δ - $[\text{Co}(\text{stn})](\text{ClO}_4)_3$ taken in a hexachlorobutadiene matrix was very similar to that in aqueous solution. The structural parameters of three tn rings of $[\text{Co}(\text{stn})]^{3+}$ are remarkably uniform, whereas those of the other six-membered chelates are all scattered (see above). In view of the fact that such scatters have been attributed¹⁷⁻²⁰ to the flexibility of six-membered chelate rings, the uniformity of conformational parameters of $[\text{Co}(\text{stn})]^{3+}$ may be regarded as suggesting the rigidity of chelate rings. Also, the NMR spectrum of $[\text{Co}(\text{stn})]^{3+}$ in aqueous solution suggested⁷ a single conformation and that no

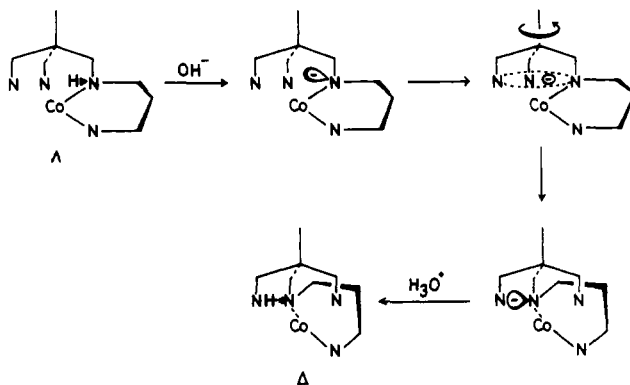


Figure 4. Possible mechanism of racemization of $[\text{Co}(\text{stn})]^{3+}$ in solution.

significant conformational change occurs even in the presence of oxyanions. Thus, it may be concluded that the conformation of $[\text{Co}(\text{stn})]^{3+}$ is locked in a flattened-chair form.

Racemization. As mentioned above, the racemization of $[\text{Co}(\text{stn})]^{3+}$ in several buffers other than collidine buffers accompanied the decomposition of the cation. The main decomposition product appeared, by electronic absorption spectra, to be a complex containing two or three oxygens as ligating atoms, with two or three arms of the stn ligand uncoordinated. Also, in solids the racemization accompanied some anation reaction for counterions Cl^- and Br^- and the bromide salt produced a trace amount of Co^{2+} as well. Thus, we admit that it may be difficult to rule out completely the possible involvement of Co-N bond breaking or Co^{2+} even in the racemization in collidine buffers, where the racemization was clean and we could not detect any hint of such effects.

The racemization of $[\text{Co}(\text{stn})]^{3+}$ in collidine buffered solution is catalyzed by OH^- . If we leave out the above possibility, we may consider that the first step of racemization is the deprotonation of amine hydrogen(s). Since coordinated secondary amine groups are usually more acidic than coordinated primary amine groups, this deprotonation may occur at a secondary amine group of $[\text{Co}(\text{stn})]^{3+}$. A most plausible mechanism leading to racemization is depicted in Figure 4. The second step of racemization will be a trigonal twist about the threefold axis of the deprotonated intermediate. This process might resemble the conventional Bailar twist at first sight, but significant difference exists. This interesting difference will be made clear if we note the following: (i) The inversion of the absolute configuration about the metal by trigonal twist should take place synchronously with the inversion of the absolute configuration of the secondary amine groups, because the chirality of the amine groups is predetermined by the chirality about the metal ion. (ii) Further, due to the presence of the interlinkage of the chelate rings, it appears requisite to invert the absolute configuration of *all* three asymmetric nitrogens simultaneously, i.e., $\Delta(\text{R},\text{R},\text{R})$ to $\Lambda(\text{S},\text{S},\text{S})$ or vice versa. In Figure 4, the second step following deprotonation is drawn so as to meet the conditions (i) and (ii) described above. In other terms, the second step may be described as a hopping of two hydrogens, or equally as a distribution of a negative charge, over three secondary nitrogens. Concurrently with this hopping, the inversion of the absolute configuration of both nitrogen and metal centers is assumed to take place. A similar distribution of a negative charge over six nitrogens was reported for the deprotonated form of $[\text{Co}(\text{sep})]^{3+}$ (sep = 1,3,6,8,10,13,16,19-octazaabicyclo[6.6.6]heptacosane).²¹

The value of activation enthalpy for racemization of $[\text{Co}(\text{stn})]^{3+}$ in solution appears quite common. The large positive entropy of activation ($+204 \pm 18 \text{ J K}^{-1} \text{ mol}^{-1}$) is considered to be consistent with the proposed deprotonated intermediate releasing water molecules of hydration upon reduction of the overall charge of the complex cation from 3+ to 2+. Large positive values of

(17) Nagao, R.; Marumo, F.; Saito, Y. *Acta Crystallogr., Sect. B: Struct. Crystallogr. Cryst. Chem.* **1973**, *B29*, 2438-2443.

(18) Sato, S.; Saito, Y. *Acta Crystallogr., Sect. B: Struct. Crystallogr. Cryst. Chem.* **1978**, *B34*, 420-425.

(19) Kobayashi, A.; Marumo, F.; Saito, Y. *Acta Crystallogr., Sect. B: Struct. Crystallogr. Cryst. Chem.* **1972**, *B28*, 3591-3595.

(20) Kobayashi, A.; Marumo, F.; Saito, Y. *Acta Crystallogr., Sect. B: Struct. Crystallogr. Cryst. Chem.* **1973**, *B29*, 2443-2447.

(21) Sugimoto, H.; Hataoka, H.; Mori, M. *J. Chem. Soc., Chem. Commun.* **1982**, 1301-1302.

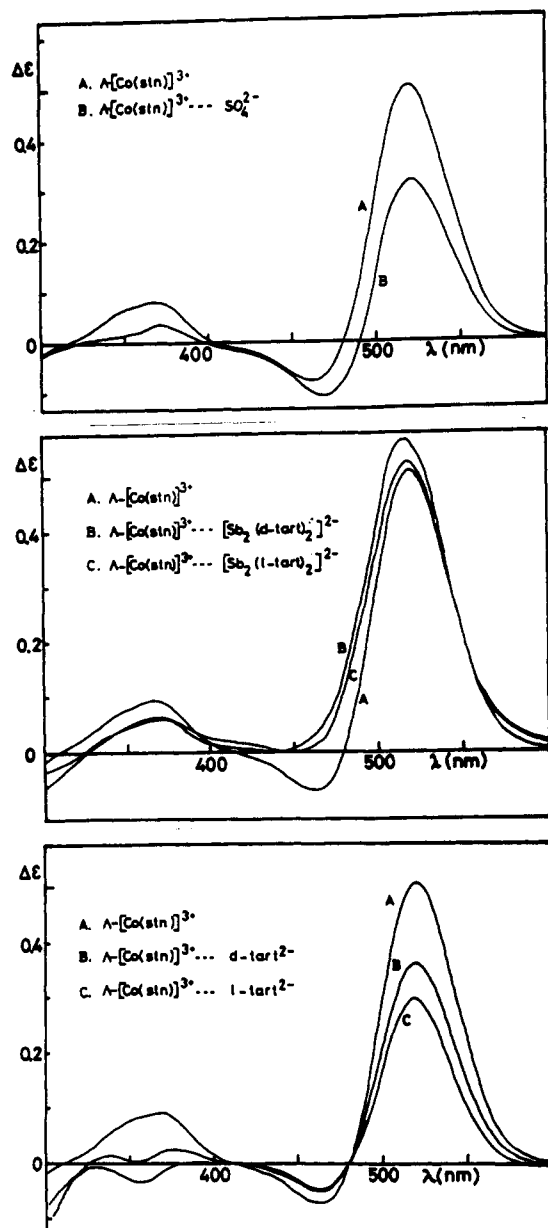


Figure 5. CD spectra of Δ -[Co(stn)]³⁺ and ion-paired species (B and C).

activation entropy have often been reported²² for the racemization of coordinated asymmetric nitrogen centers, which proceeds also upon deprotonation.

In the solid state, the racemization proceeded in two stages. The initial rapid loss of optical activity may be related to the racemization accelerated by a rearrangement of crystal lattices²³ or by an annealing process of crystal defects.²⁴ The second slower process may be the racemization in the crystal lattice thus formed. However, the true nature of these processes is not clear as yet. Since, in the crystal, deprotonation is unlikely and a large negative entropy of activation was obtained for the slower process, in contrast to a large positive value in solution, the racemization in the solid state may proceed by a somewhat different mechanism. Our guess is a trigonal twist wherein the nitrogen inversion is effected by rupture of Co–N bonds, though the possible involvement of Co²⁺ may not be eliminated. Though geometrical

isomerization and racemization of [Co(N)₆]³⁺ complexes are not totally unprecedented, it seems worthwhile to comment on the origin of this facile racemization. Also, the facile racemization of [Co(stn)]³⁺ contrasts with the inertness of the parent [Co(tn)]³⁺ under similar conditions. As noted above, the structure of [Co(stn)]³⁺ is rather strained owing to the trimethyleneethane capping, especially in the vicinity of secondary asymmetric nitrogens. The cobalt(III) complexes of symmetrical hexaaza macrocycles synthesized recently by Royer et al.²⁵ are reported to racemize and isomerize easily. A common structural feature of their complexes and [Co(stn)]³⁺ is a severe steric strain imposed by interlinkages between chelate rings. Thus, the facile racemization of [Co(stn)]³⁺ may be considered to result from steric strain. Recently, we showed that the steric strain in [Co(N)₆]³⁺ hexaamine complexes increases the Co–N bond length and hence decreases the crystal field splitting parameter (10Dq), leading to a red shift in the absorption spectrum.³ Therefore, in Co(III) complexes, one of the effects of steric strain may be considered to be the elongation and hence weakening of Co–N bonds. This idea seems to be supported by the successful application of strain-energy minimization (or molecular mechanics) calculations²⁶ to Co(III) complexes in reproducing structural features. Evidence for the weakened Co–N bonds in [Co(stn)]³⁺ has been provided by several lines of observations, as described above.

Ion Association. The effect of ion association upon the CD spectrum of Δ -[Co(stn)]³⁺ was examined qualitatively by Hermer and Douglas.⁷ The CD changes brought about by sulfate and bis(μ -tartrato)diantimonate(III) ions are in such a direction that they enhance the A₂ and E_a rotational strengths, respectively (see Figure 5). For complexes with five-membered chelate rings and an effective D₃ symmetry, the following idea is known²⁷ to work very well. Perturbations along the D₃ axial and equatorial directions enhance generally the A₂ and E_a rotational strengths, respectively. If we apply this idea to the CD changes in Figure 5, the sulfate and bis(μ -tartrato)diantimonate(III) ions may be considered to associate along the axial and equatorial directions of [Co(stn)]³⁺, respectively. Such directions of ion association of these ions coincide with the results of previous studies;^{2,28} for example, the sulfate ion approaches the [Co(en)₃]³⁺ type of cations along the C₃ direction and forms a triple hydrogen bond with three NH hydrogens.²⁸ Thus, the above ideas seems to hold also for complexes with six-membered chelate rings in a chair₃ conformation. The origin of anomalous CD changes due to *d*- and *l*-tartrate ions is not clear.

The degree of chiral discrimination, as defined by 100(K_d – K_l)/(K_d + K_l), for tartrate systems is rather high (about 30%), where K_d and K_l are the K values of Δ -[Co(stn)]³⁺ for *d* and *l* isomers. For comparison, the degrees of chiral discrimination in [Co(en)₃]³⁺, [Co(sen)]³⁺, and [Co(sep)]³⁺ are 7, 18, and 0%, respectively.² The high degree of chiral discrimination found here also suggests that the conformation of chelate rings is locked in solution. The fact that K_d is larger than K_l indicates that the Δ cation prefers the *d*-tartrate and bis(μ -*d*-tartrato)diantimonate(III) ions. This preference is consistent with the results of ion-exchange chromatography on SP-Sephadex C-25; sorption of racemic [Co(stn)]³⁺ on the resin and elution with *d*-tartrate and bis(μ -*d*-tartrato)diantimonate(III) solutions led to a faster desorption of Δ -[Co(stn)]³⁺.

Supplementary Material Available: Final atomic coordinates for hydrogen atoms with isotropic thermal parameters (Table II), final anisotropic thermal parameters for non-hydrogen atoms (Table III), hydrogen bond distances (Table VI), and a listing of observed and calculated structure factor amplitudes (25 pages). Ordering information is given on any current masthead page.

- (22) (a) Buckingham, D. A.; Marzilli, L. G.; Sargeson, A. M. *J. Am. Chem. Soc.* **1967**, *89*, 825–830. (b) Halpern, B.; Sargeson, A. M.; Turnbull, K. R. *J. Am. Chem. Soc.* **1966**, *88*, 4630–4636. (c) Buckingham, D. A.; Marzilli, L. G.; Sargeson, A. M. *J. Am. Chem. Soc.* **1967**, *89*, 3428–3433.
 (23) Kutal, C.; Bailar, J. C. *J. Phys. Chem.* **1972**, *76*, 119–127.
 (24) Chowdhury, D. M.; Harris, G. M. *J. Phys. Chem.* **1969**, *73*, 3366–3369.

- (25) Royer, D. J.; Grant, G. J.; Van Derfveer, D. G.; Castillo, M. *J. Inorg. Chem.* **1982**, *21*, 1902–1908.
 (26) See, for example: Taylor, S. G.; Snow, M. R.; Hambley, T. W. *Aust. J. Chem.* **1983**, *36*, 2359–2368 and references cited therein.
 (27) Drake, A. F.; Kuroda, R.; Mason, S. F. *J. Chem. Soc., Dalton Trans.* **1979**, 1095–1100.
 (28) (a) Ogino, K.; Saito, U. *Bull. Chem. Soc. Jpn.* **1967**, *40*, 826–829. (b) Taura, T.; Yoneda, H. *Inorg. Chem.* **1978**, *17*, 1495–1498.